Macromolecules

Volume 37, Number 22 November 2, 2004

© Copyright 2004 by the American Chemical Society

Communications to the Editor

Cocrystallization Behavior in Binary Blend of Crystalline−Amorphous Diblock Copolymers

Yen-Yu Huang,[†] Bhanu Nandan,[†] Hsin-Lung Chen,*[,†] Chien-Shiun Liao,[‡] and U-Ser Jeng[§]

Department of Chemical Engineering, National Tsing Hua University, Hsin-Chu, Taiwan 30013, R.O.C.; Department of Chemical Engineering, Yuan Ze University, Nei-Li, Taoyuan, Taiwan 320, R.O.C.; and National Synchrotron Radiation Research Center, Hsin-Chu, Taiwan 300, R.O.C.

Received May 19, 2004
Revised Manuscript Received September 21, 2004

Fractionation during crystallization of heterodisperse homopolymers is a well-known phenomenon that originates from the mixing gap in the crystalline state of chain molecules differing sufficiently in length. Under thermodynamic equilibrium conditions, a binary mixture of homologous chain molecules with large disparity in molecular weights solidifies to form two solid phases. Under nonequilibrium conditions, however, solid solutions may form at relatively low solidification temperatures where the crystallization proceeds so rapidly that the cross-diffusion of the molecules, which is an essential step in the fractionation, is impeded.[1]

Recently, much attention has been paid to crystalline−amorphous diblock copolymers (C-*b*-A) and their blends with homopolymer A because their self-assembled structures provide interesting templates to explore the crystallization behavior of polymer chains confined in nanoscale space once C block forms microdomains in the melt state.[2−5] In this study, we will deal with the blends of two chemically identical C-*b*-A with different chain lengths, i.e., C_α-*b*-A_β/C_γ-*b*-A_δ with the subscript representing the degree of polymerization. Though the binary blends of diblock copolymers have received considerable theoretical and experimental interests due to richness of their phase behavior, most of the works have been carried out on systems with all amorphous blocks.[6−12] Introduction of a crystallizable block into this type of system is expected to create more complex phase behavior than normally has been observed for their amorphous counterparts. A very important question which arises naturally is whether C_α and C_γ blocks originally mixed within the microdomains in the melt would cocrystallize or phase segregate into their own crystalline lamellar structures. In this study, we intend to demonstrate that cocrystallization leading to a solid solution occurs over a broad range of undercooling in the lamellae-forming blends of a nearly symmetric C-*b*-A with an asymmetric counterpart, while the corresponding homopolymer blends with similar molecular weight and compositions exhibit phase-segregated crystallization. In contrast to the kinetically trapped solid solution formed in homopolymer system, the cocrystallization of C_α and C_γ blocks may be driven thermodynamically by the tendency of A_β and A_δ blocks to remain intimately mixed.

The system under study is the blends of a short nearly symmetric poly(ethylene oxide)-*block*-polybutadiene (PEO-*b*-PB) and a long asymmetric PEO-*b*-PB with PEO and PB being the crystalline and amorphous blocks, respectively. The nearly symmetric PEO-*b*-PB (denoted as $E_{170}B_{102}$) had the number-average molecular weight of the respective blocks as $M_{b,PEO} = 7500$ and $M_{b,PB} = 5500$. $M_{b,PEO}$ and $M_{b,PB}$ of the asymmetric PEO-*b*-PB (denoted as $E_{80}B_{481}$) were 3500 and 26 000, respectively. The melt morphology of neat $E_{170}B_{102}$ and $E_{80}B_{481}$ is lamellae and BCC-packed PEO spheres, respectively. $E_{80}B_{481}/E_{170}B_{102}$ blends were prepared by solution mixing using toluene as the solvent. The compositions of the blends are designated as the weight ratio of $E_{80}B_{481}$ to $E_{170}B_{102}$. The blends of two PEO homopolymers with approximately the same molecular weights as those of the PEO blocks in the copolymer blends were also prepared for comparing the crystallization behavior of

[†] National Tsing Hua University.
[‡] Yuan Ze University.
[§] National Synchrotron Radiation Research Center.
* To whom correspondence should be addressed.

10.1021/ma049012l CCC: $27.50 © 2004 American Chemical Society
Published on Web 10/06/2004

Table 1. Characteristics of the Binary Diblock Copolymer Blends Studied in This Work

$E_{80}B_{481}$/ $E_{170}B_{102}$ (in wt %)	weight ratio of E_{80} and E_{170} blocks in the PEO domain[a]	f_{PEO}[b]	melt structure of PEO domain
0/100	0/100	0.54	lamellae
20/80	1/19	0.45	lamellae
40/60	1/7	0.36	lamellae
50/50	1/5	0.32	lamellae
55/45	1/4	0.29	lamellae
100/0	100/0	0.10	sphere

[a] The compositions of homopolymer mixtures (h-E_{76}/h-E_{182}) were based on this ratio. [b] Overall volume fraction of the PEO block.

PEO in these two types of systems. The PEO homopolymers with $M_{h,PEO} = 3350$ (denoted as h-E_{76}) and $M_{h,PEO} = 8000$ (denoted as h-E_{182}) were purchased from Sigma. The h-E_{76}/h-E_{182} blend compositions were based on the calculated weight ratios of the two PEO blocks in the PEO domain of the copolymer mixtures (cf. Table 1).

First we would like to verify that the shorter and the longer PEO/PB blocks in $E_{170}B_{102}$ and $E_{80}B_{481}$ mix intimately in their respective microdomains in the melt state. Figure 1a shows a series of small-angle X-ray scattering (SAXS) profiles obtained in the melt state from $E_{80}B_{481}/E_{170}B_{102}$ blends with the weight percent of $E_{80}B_{481}$ up to 55%. Each profile is characterized by a primary scattering peak along with the higher-order maxima situating at integer multiples of the first-order peak position, which clearly indicates the formation of lamellar morphology in these blends. Figure 1b plots the interlamellar distance (D) and the area per junction point at the lamellar interface (Σ) as a function of the number fraction of the asymmetric $E_{80}B_{481}$ (n_{as}). The interfacial area per junction was obtained from[12]

$$\Sigma = 2\{[(1 - n_{as})N_{s,PB} + n_{as}N_{as,PB}]v_{PB} + [(1 - n_{as})N_{s,PEO} + n_{as}N_{as,PEO}]v_{PEO}\}/D \quad (1)$$

where $N_{s,i}$ and $N_{as,i}$ (with i = PB or PEO) is the degree of polymerization of i block in $E_{170}B_{102}$ and $E_{80}B_{481}$, respectively, and v_i is the volume of an i monomer unit ($v_{PB} = 0.095$ nm^3 and $v_{PEO} = 0.072$ nm^3). It can be seen that the interlamellar distance increases with increasing fraction of $E_{80}B_{481}$, whereas Σ remains constant and equals approximately to that in neat $E_{170}B_{102}$. The observed composition dependences of D and Σ are in parallel with those exhibited by the blends of a short symmetric polystyrene-*block*-polyisoprene (PS-*b*-PI) and a long asymmetric PS-*b*-PI reported by Court and Hashimoto.[11,12] The swelling of interlamellar distance upon adding $E_{80}B_{481}$ indicates that the bipopulated PEO/PB blocks mix intimately in their respective domains, where the much longer PB blocks from $E_{80}B_{481}$ effectively swells the thickness of PB lamellae. The interfacial area per junction point is however dominated by the short symmetric diblock as manifested by the proximity of Σ to that in neat $E_{170}B_{102}$ irrespective of the blend composition. In this case, each lamellar domain (PB in particular) is constituted of two layers of brushes lying on top of each other. The first layer is formed by the shorter blocks and the first subchains in the longer blocks, while the second layer composes of the remaining subchains of the longer blocks, as illustrated in Figure 2a.[12]

The intimate mixing of the block chains in the respective domains is further supported by the suppression of the third-order diffraction peak for 40/60, 50/50, and 55/45 blends (cf. Figure 1a), in which the overall volume fraction of PEO (f_{PEO}) lies in the vicinity of 0.3 (cf. Table 1). As the intensity of the nth-order diffraction from the lamellar array is proportional to $\sin^2(n\pi f_{PEO}{}^L)$, with $f_{PEO}{}^L$ being the volume fraction of PEO lamellae in the array, the diminishment of the third-order peak means that $f_{PEO}{}^L$ is close to $^1/_3$. The proximity between f_{PEO} prescribed by the feed ratio and $f_{PEO}{}^L$ attests that the lamellar stacks are formed by the uniform mixing of the two diblocks. The intimate mixing is favored because the resultant lamellar structure has a lower interfacial energy (compared with the macrophase-separated state containing the spherical domains formed by $E_{80}B_{481}$), while allowing the long PB blocks in $E_{80}B_{481}$ to relax conformationally in the lamellar domains according to the chain packing mode depicted in Figure 2a.

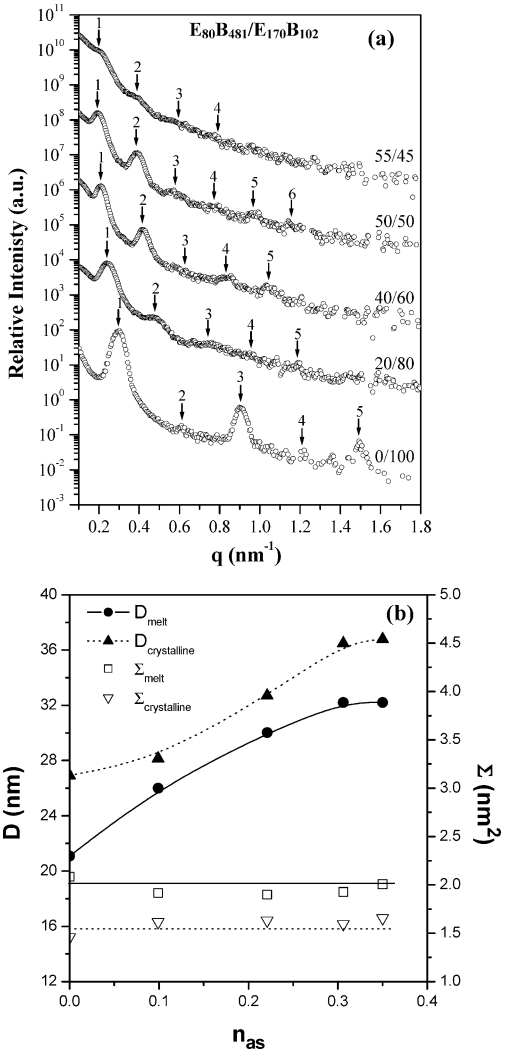

Figure 1. (a) SAXS profiles of lamellae-forming $E_{80}B_{481}/E_{170}B_{102}$ blends in the melt state. The SAXS experiments were conducted at 90 °C. (b) Variations of the interlamellar distance (D) and the area per junction point at the lamellar interface (Σ) with the number fraction of the asymmetric $E_{80}B_{481}$ (n_{as}) for the blends in melt and crystalline (T_c = 40 °C) states.

The cocrystallization or phase-segregated crystallization phenomenon in the diblock and homopolymer blends is revealed from the melting behavior of the samples isothermally crystallized at different temperatures (T_c). The representative DSC melting curves of h-E_{76}/h-E_{182} and $E_{80}B_{481}/E_{170}B_{102}$ blends subjected to isothermal crystallization at 8 °C (high undercooling)

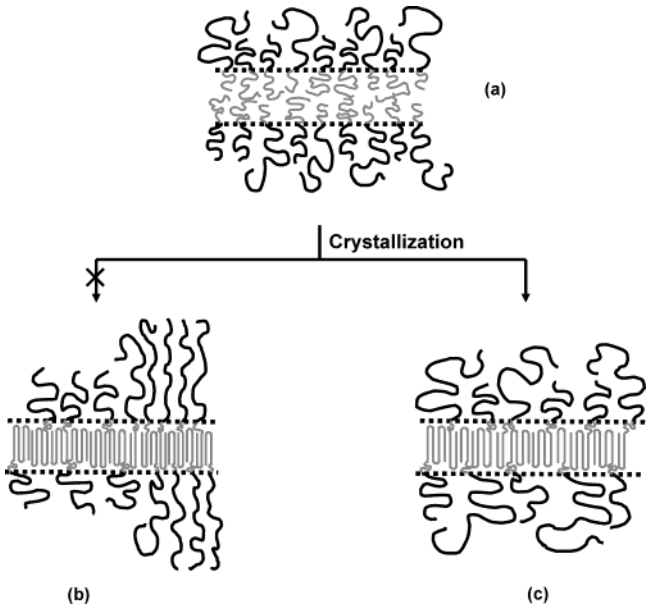

Figure 2. Schematic illustrations of the structures of $E_{80}B_{481}/E_{170}B_{102}$ blend. (a) Melt structure formed by the intimate mixing of the two diblocks, where each lamellar domain is constituted of two layers of brushes lying on top of each other. (b) Crystalline structure generated by the phase-segregated crystallization, where the crystallites formed by the longer and shorter PEO blocks coexist within the lamellar domains upon fractionation. The long PB blocks are highly stretched to maintain the normal density in the PB domain. (c) Crystalline structure generated by cocrystallization. This structure allows the lower interfacial energy and higher conformational entropy of the long PB blocks in the melt state to be largely retained.

and 40 °C (low undercooling) are displayed in Figure 3. From Figure 3a,b, it can be observed that most homopolymer mixtures show two melting endotherms irrespective of T_c, one of which is present as a shoulder to the main peak. The two melting peaks correspond to those of the pure homopolymers and hence reveal a fractionation process during crystallization in the binary mixtures. The 1/19 blend tends to display a single endotherm upon crystallization at 8 °C, which may be due to the formation of a kinetically trapped solid solution in this dilute mixture at high undercooling. The molecular weight fractionation during crystallization in the binary mixtures of PEO homopolymers has been well described in the past.[13−15] Though the phase-segregated crystallization behavior at low undercooling such as at 40 °C (cf. Figure 3b) is quite typical from the literature reports, that observed at relatively high undercooling (cf. Figure 3a) is rather unexpected. This shows that the blends of relatively low molecular weight PEO have a strong tendency toward fractionation during crystallization.

The melting curves of $E_{80}B_{481}/E_{170}B_{102}$ blends are displayed in Figure 3c,d. It is noted that the melting curve of neat sphere-forming $E_{80}B_{481}$ shown for comparison was obtained after cooling the sample to −50 °C because crystallization of PEO blocks from the spherical domains must predominantly involve homogeneous nucleation which takes place at very large undercooling (ΔT > 90 K).[2,3] Contrary to the observed behavior for homopolymer blends, the diblock copolymer mixtures exhibit a single melting endotherm for crystallization at both low and high undercoolings, and the peak temperature decreases as the concentration of $E_{80}B_{481}$ increases. This implies that the shorter and the longer PEO blocks in $E_{80}B_{481}$ and $E_{170}B_{102}$, respectively, *cocrystallize* in the lamellar microdomains irrespective of the composition and the degree of undercooling. Nevertheless, considering that the longer E_{170} blocks may tend to crystallize first, this crystallization could induce a macrophase separation through which the asymmetric $E_{80}B_{481}$ is segregated to form PEO spherical microdomains before the shorter E_{80} blocks have a chance to crystallize. Once the spherical domains are formed, the E_{80} blocks confined within them are no longer crystallizable at the prescribed crystallization temperatures; in this case, the isothermally crystallized diblock blends will still exhibit a single melting endotherm associated solely with $E_{170}B_{102}$. This scenario is however ruled out from the fact that the heat of melting of the endotherm observed in Figure 3c,d varies linearly with the overall weight fraction of PEO in the diblock blend, which attests that the melting peak is contributed by the crystallinities of both E_{170} and E_{80} blocks. Moreover, we have annealed the isothermally crystallized blends at −50 °C for 48 h because in the event of the crystallization-induced macrophase separation this low-temperature treatment would be sufficient to crystallize the E_{80} blocks in the spherical microdomains, such that the subsequent heating curves should show *two* melting endotherms. The heating curves recorded after such a treatment however produces only a single endotherm for all compositions and are virtually identical with those shown in Figure 3c,d. This emphatically proves that the observed single endotherm signals cocrystallization of the shorter and the longer PEO blocks in the copolymer blends.

Cocrystallization in the diblock blends is also supported by the SAXS profiles of the isothermally crystallized samples, as presented in Figure 4 for T_c = 40 °C. The salient features of the scattering profiles of the molten blends (cf. Figure 1a) are seen to retain after the crystallization, where a series of lamellar peaks are observed with the peak position shifting to lower q with increasing concentration of $E_{80}B_{481}$. The interlamellar distance and the cross-sectional area per junction point of the crystalline blend are also plotted as a function of n_{as} in Figure 1b. At a given composition D and Σ increase and decrease upon crystallization, respectively, because the tighter packing of PEO chains in the crystals reduces Σ and hence results in a higher stretching of the PB blocks. The fact that the variations of D and Σ with n_{as} follow the same trends as those associated with the molten blends indicates that the bipopulated PEO/PB blocks remain intimately mixed in their respective domains and hence provides further evidence for cocrystallization of the shorter and the longer PEO blocks.

We now consider why the diblock blends tend to cocrystallize while fractionation is favored during crystallization in the corresponding homopolymer blends. Intuitively, phase-segregated crystallization will not be allowed if microdomain A in the copolymer blend is vitrified at T_c (i.e., T_g of A block > T_c) because the immobility of junction points at domain interface prohibits any cross-diffusion involved in the fractionation of C blocks. This condition however does not apply here since the T_c's under study are well above the T_g of PB. Since PEO and PB blocks are covalently connected, fractionation of PEO blocks will invariably demix the short and long diblocks in the blends. The interfacial

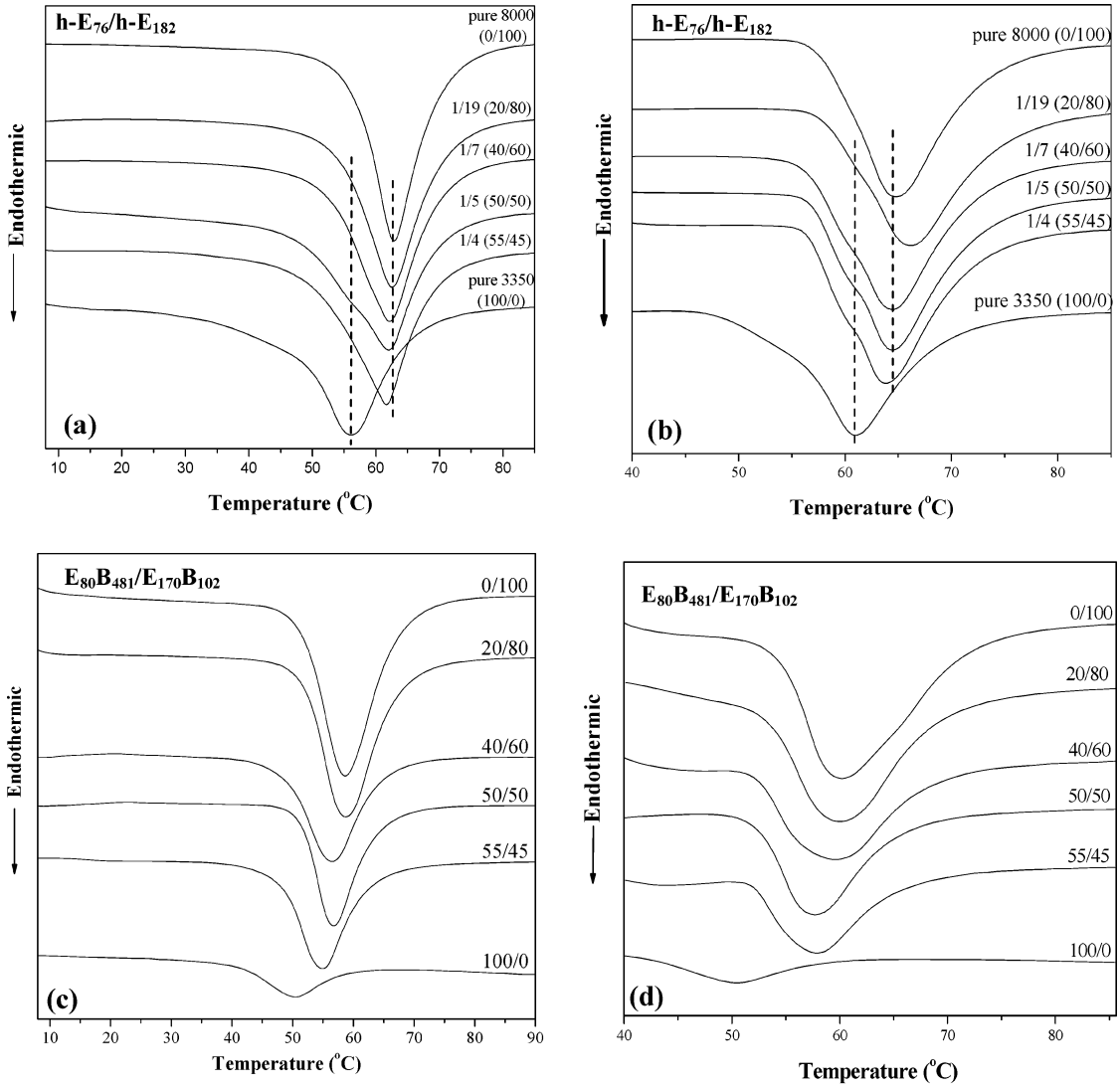

Figure 3. DSC melting curves of h-E_{76}/h-E_{182} and $E_{80}B_{481}/E_{170}B_{102}$ blends obtained after isothermal crystallization at a heating rate of 20 °C/min: (a) h-E_{76}/h-E_{182}, T_c = 8 °C; (b) h-E_{76}/h-E_{182}, T_c = 40 °C; (c) $E_{80}B_{481}/E_{170}B_{102}$, T_c = 8 °C; (d) $E_{80}B_{481}/E_{170}B_{102}$, T_c = 40 °C. Each bracket in (a) and (b) indicates the corresponding composition of the diblock blend with the same mixing ratio of the shorter and the longer PEO chains as that in the homopolymer blend. The melting curves of neat $E_{80}B_{481}$ in (c) and (d) were obtained after cooling the sample to −50 °C.

energy of the system will increase if the asymmetric $E_{80}B_{481}$ demixing from the crystallizing symmetric $E_{170}B_{102}$ reassembles into spherical micelles. Therefore, phase-segregated crystallization will not be thermodynamically favored once the reduction of the free energy of crystalline PEO phase from fractionation cannot compensate the gain in interfacial energy. The increase of interfacial energy may in principle be circumvented if the fractionation process is confined within the preexisting lamellar microdomains, where the crystallites formed by the longer and shorter PEO blocks coexist within the lamellar domains upon fractionation, as illustrated in Figure 2b. However, this lamellar structure contains an entropic penalty due to excessive stretching of the long PB blocks. In light of the energetic and entropic penalties introduced by phase-segregated crystallization, the cocrystallized structure shown in Figure 2c,[16] in which the shorter and the longer PEO blocks cocrystallize uniformly in the microdomain with similar lamellar thickness, may become the thermodynamically favored morphology of the system. In other words, it is plausible that the cocrystallization of PEO blocks is driven *thermodynamically* by the tendency of the short and long PB blocks to remain intimately mixed to reduce the interfacial energy between PEO and PB phases while allowing the long PB blocks in the asymmetric diblock to relax conformationally.

In summary, we have shown that the PEO blocks of different lengths in the binary PEO-*b*-PB blends tended to cocrystallize whereas the corresponding blends of PEO homopolymers showed phase-segregated crystallization. In contrast to the kinetically trapped solid solutions formed in homopolymer systems, cocrystallization in the present blends may be driven thermodynamically by the tendency of the short and long PB blocks to remain intimately mixed. The cocrystallization observed here represents a scenario where a kinetics-dominated process found in homopolymer crystallization possibly turns into a thermodynamically favored process in the C-*b*-A systems. Another example is the crystalline chain folding; chain folding during crystallization in homopolymer is a kinetically driven phenomenon, whereas in diblock copolymers chain folding in the

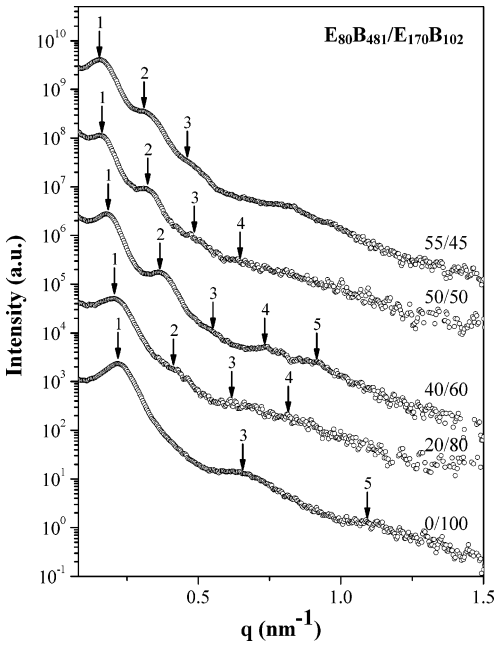

Figure 4. SAXS profiles of $E_{80}B_{481}/E_{170}B_{102}$ blends isothermally crystallized at 40 °C.

crystalline domain may be thermodynamically driven to enlarge the cross section per junction point to avoid excessive stretching of the A block chains.[17,18]

Acknowledgment. This work was supported by the National Science Council of R.O.C. under Grant NSC92-2216-E-110-009 and also in part by the National Synchrotron Radiation Research Center under Project ID 2003-3-037.

References and Notes

(1) Smith, P.; Manley, R. *Macromolecules* **1979**, *12*, 483.
(2) Chen, H.-L.; Hsiao, S.-C.; Lin, T.-L.; Yamauchi, K.; Hasegawa, H.; Hashimoto, T. *Macromolecules* **2001**, *34*, 671.
(3) Chen, H.-L.; Wu, J.-C.; Lin, T.-L.; Lin, J. S. *Macromolecules* **2001**, *34*, 6936.
(4) Loo, Y.-L.; Register, R. A.; Ryan, A. J.; Dee, G. T. *Macromolecules* **2001**, *34*, 8968.
(5) Xu, J.-T.; Fairclough, J. P. A.; Mai, S.-M.; Ryan, A. J.; Chainbundit, C. *Macromolecules* **2002**, *35*, 6937.
(6) Shi, A.-C.; Noolandi, J. *Macromolecules* **1994**, *27*, 2936.
(7) Hashimoto, T.; Koizumi, S.; Hasegawa, H. *Macromolecules* **1994**, *27*, 1562.
(8) Shi, A.-C.; Noolandi, J. *Macromolecules* **1995**, *28*, 3103.
(9) Zhao, J.; Majumdar, B.; Schulz, M. F.; Bates, F. S.; Almdal, K.; Mortensen, K.; Hajduk, D. A.; Gruner, S. M. *Macromolecules* **1996**, *29*, 1204.
(10) Sakurai, S.; Irie, H.; Umeda, H.; Nomura, S.; Lee, H. H.; Kim, J. K. *Macromolecules* **1998**, *31*, 336.
(11) Court, F.; Hashimoto, T. *Macromolecules* **2001**, *34*, 2536.
(12) Court, F.; Hashimoto, T. *Macromolecules* **2002**, *35*, 2566.
(13) Prud'homme, R. E. *J. Polym. Sci., Part B: Polym. Phys.* **1982**, *20*, 307.
(14) Cheng, S. Z. D.; Wunderlich, B. *J. Polym. Sci., Part B: Polym. Phys.* **1986**, *24*, 577. (b) Cheng, S. Z. D.; Wunderlich, B. *J. Polym. Sci., Part B: Polym. Phys.* **1986**, *24*, 595. (c) Cheng, S. Z. D.; Wunderlich, B. *J. Polym. Sci., Part B: Polym. Phys.* **1988**, *26*, 1947.
(15) Balijepalli, S.; Schultz, J. M.; Lin, J. S. *Macromolecules* **1996**, *29*, 6601.
(16) The model structures are drawn based on the SAXS results of the isothermally crystallized diblock blends from which the PEO lamellar thickness was calculated to be ca. 10.8 nm. Assuming that crystalline stems orient perpendicular to the interface,[17] this gives a once folded and triply folded chain structure for the shorter (extended chain length = 22.15 nm) and the longer (extended chain length = 47.47 nm) PEO blocks in $E_{80}B_{481}$ and $E_{170}B_{102}$, respectively.
(17) DiMarzio, E. A.; Guttman, C. M.; Hoffman, J. D. *Macromolecules* **1980**, *13*, 1194.
(18) Whitmore, M. D.; Noolandi, J. *Macromolecules* **1988**, *21*, 1482.

MA049012L